Available online at www.sciencedirect.com
SCIENCE DIRECT®
Measurement 39 (2006) 664–673
Measurement
www.elsevier.com/locate/measurement

Characterisation of frequency instability and frequency offset using instruments with incomplete data sheets

Juan José González de la Rosa [a,*], A. Moreno [b], I. Lloret [a], V. Pallarés [b], M. Liñán [b]

[a] University of Cádiz, Electronics Area, Research Group TIC168—Computational Electronics Instrumentation, EPSA Av. Ramón Puyol S/N, E-11202-Algeciras-Cádiz, Spain
[b] University of Córdoba, Department of Electronics, Spain

Received 8 December 2004; received in revised form 27 December 2005; accepted 3 January 2006
Available online 20 February 2006

Abstract

This paper describes how to deal with electronic instruments, commonly used in frequency calibrations, whose data sheets do not include complete information regarding the sources of error (uncertainties), which affect the accuracy and stability of the frequency under test. Considering a time interval counter as the measurement unit, and a GPS receiver as the traceable standard, the purpose is twofold. First, contributions to the Type B uncertainty are calculated under the assumption of uniformly distributed errors. An expression is used for frequencies under test whose values are close to 1 Hz. Secondly, short-term instability is studied using non-classical statistics, which have been previously tested using simulated data. Then, a white noise test is performed based on the calculation of the classical to non-classical variance ratio, and supported by the direct measurement of the slopes in the graphs which depicts the variances (the Allan deviation and the modified Allan deviation) vs. the measurement time.

Keywords: Allan deviation; Frequency calibrations; Frequency instability; Low-cost measurements; Modified Allan deviation; Non-classical statistics; Noise processes; Short-term stability; Type B uncertainty; Uncertainty calculations

1. Introduction

Time interval counters and GPS receivers (as transfer standard lab sources) are widely used in traceable frequency calibrations. The transfer standard receives a signal, which has been previously generated by a caesium-oscillator-based system, subsequently conferring high stability to the reference frequency delivered by the lab source. This caesium-derived frequency is available to the user, who is benefited, as not all laboratories can afford a caesium [1–3]. These instruments differ in specifications and details regarding the time base, the main gate and the counting assembly. Furthermore, manufacturers tend to omit the conditions under these specifications have been provided or measured. The instruments often are supplied with data sheets

* Corresponding author. Tel.: +34 9560 28020; fax: +34 9560 28001.
E-mail address: juanjose.delarosa@uca.es (J.J. González de la Rosa).

0263-2241/$ - see front matter
doi:10.1016/j.measurement.2006.01.001

lacking in details concerning the probability density function of the errors. Moreover, information concerning some types of uncertainty is missing in their data sheets.

Frequency calibrations involve the calculation of the frequency offset, and the characterisation of the noise process which mostly affects the short-term stability of the frequency source under test. Consequently, assumptions have to be made in order to perform a frequency calibration using these incompletely characterised electronic instruments.

Considering a medium-cost time interval counter as the measurement unit, and a GPS receiver as the traceable standard, the paper shows how to calibrate a function generator which delivers a frequency, whose value is close to 1 Hz. Based on this experience, the purpose of the paper is twofold. First, contributions to the Type B uncertainty (via the sensitivity coefficients in the error propagation expression) are calculated under the assumption of dealing with errors which exhibit rectangular probability distributions. An expression is considered for frequencies under test whose values are close to 1 Hz. The value for the measured frequency and its associated uncertainty is then reported, considering uncertainties of Types A and B. It is shown that Type A uncertainty degrades in one order of magnitude the Type B uncertainty, which is of 1 part in 10^7.

Secondly, short-term instability is studied in a simulated scenario, using non-classical statistics (Allan deviations estimates) which have been previously tested using noise processes, which in turn have been modelled using a seed function based on the five power spectral laws. A result regarding the simultaneous action of two noise processes is reported to show that it is possible to have a low-variance noise masked by a higher variance one. These pre-experimental calculations are thought to assess the performance of the non-classical statistics compared to the results found in: [4–8]. Then, going back to the experimental case, a white noise test is performed based on the calculation of the classical to non-classical variance ratio [9], and supported by the direct measurement of the slopes in the graphs which depict the Allan deviation and the modified Allan deviation vs. the measurement time.

The paper is organised as follows: Section 2 shows the details concerning the calculation of the standard uncertainty associated to the frequency measurement; the error propagation expressions and types of uncertainty are revised; then a wide-spread expression [9] for the calculation of frequencies which are close to 1 Hz is adopted to calculate the sensitivity coefficients which contribute to the standard uncertainty. In Section 3, the five independent noise processes which commonly affect oscillators are revised, along with the non-classical deviations (Allan deviations) which allow their identification. The experience is described in Section 4, and the conclusions are drawn in Section 5.

2. Uncertainty propagation using a reference signal of 1 pps

2.1. Sensitivity coefficients

In calibration we usually deal with a measurand, Z, which is the particular quantity subject to the measurement and is considered as the output of the measurement system. This quantity depends upon a set of input random variables X_i according to a functional relationship given by a function f, representing the procedure of the measurement and the method of evaluation [10,11]

$$Z = f(X_1, X_2, \ldots, X_N). \tag{1}$$

An estimate of the measurand, denoted by z, is obtained from Eq. (1) using input estimates x_i

$$z = f(x_1, x_2, \ldots, x_N). \tag{2}$$

The standard uncertainty associated with that estimate $u(z)$, depends on the particular uncertainties of the input quantities $u(x_i)$. For uncorrelated input quantities the square of the standard uncertainty of the output estimate is given by

$$u^2(z) = \sum_{i=1}^{N} u_i^2(z), \tag{3}$$

where the individual contributions in Eq. (3) are obtained through the sensitivity coefficients c_i via

$$u_i(z) = c_i u(x_i), \quad c_i = \left[\frac{\partial f}{\partial X_i}\right]_{x_i}. \tag{4}$$

2.2. Types of uncertainty for the input estimates

The uncertainty of measurement associated with the input estimates is evaluated according to different methods of evaluation. The Type A evaluation of standard uncertainty is the method which considers the statistical analysis of a series of observations. The standard uncertainty is the experimental

standard deviation of the mean, which in turn results from a regression analysis. By the contrary, the Type B method is based on scientific knowledge [10,11].

The standard uncertainty of one input estimate $u(x_i)$, evaluated via the Type B method, comprises all the information related to the variability of the measurand X_i. This variability can fall into the following six categories:

- previous measurements;
- general knowledge of the behaviour and properties of relevant materials and instruments;
- manufacturer's specifications;
- data provided in calibration certificates;
- uncertainties assigned to reference data in handbooks.

As a consequence, insight and general knowledge are the sources of information for a Type B evaluation of standard uncertainty. The electronics instruments involved in this experience are not provided with detailed data sheets, with the uncertainties associated to the quantities X_i. Only upper and lower limits can be estimated for the values of the quantities in the manufacturer's specifications. Thus, it has to be assumed a constant probability density between these limits. A rectangular probability distribution is a reasonable description of one's inadequate knowledge about an input quantity in absence of any other information apart from its limits of variability.

2.3. The measurand in traceable frequency characterisation

In traceable frequency calibrations the expression for the measurand f_{meas} is given by

$$f_{\text{meas}} = \left[\frac{1}{\frac{1}{f_{\text{REF}}} \pm \frac{\Delta x}{\tau}}\right]_{f_{\text{REF}},\overline{\Delta x},\tau} = \left[\frac{f_{\text{REF}}}{1 \pm f_{\text{REF}}\frac{\Delta x}{\tau}}\right]_{f_{\text{REF}},\overline{\Delta x},\tau}, \tag{5}$$

where f_{REF} is the reference (1 pps), Δx represents the incremental phase shift between the source under test and the reference, and τ is the averaging time of the measurement system. Eq. (5) is evaluated in the averaged phase shift during the calibration period. For a zero phase shift, or an infinity averaging time, looking at Eq. (5), we have the ideal case ($f_{\text{meas}} = f_{\text{REF}}$).

Using Eqs. (3)–(5), the uncertainty of the frequency is obtained from Eq. (6) via

$$u^2(f_{\text{meas}}) = \left(1 - f_{\text{REF}}\frac{\overline{\Delta x}}{\tau}\right)^{-4} \times [u^2(f_{\text{REF}}) + u^2(\Delta x) + u^2(\tau)]. \tag{6}$$

Sensitivity coefficients in Eqs. (3) and (4) determine the contributions of the Type B uncertainty, which is associated to the instrument's specifications.

3. Classical noise models

3.1. Characterising instabilities

It is a customary situation to deal with unperfect signals which contain additive noise. The instantaneous output voltage of an oscillator can be expressed as

$$v(t) = [V_0 + \varepsilon(t)]\sin[2\pi v_0 t + \phi(t)], \tag{7}$$

where V_0 is the nominal peak voltage amplitude, $\varepsilon(t)$ is the deviation from the nominal amplitude, v_0 is the name-plate frequency, and $\phi(t)$ is the phase deviation from the ideal phase $2\pi v_0 t$. Changes in the peak value of the signal is the amplitude instability. Fluctuations in the zero crossings of the voltage is the phase instability. The so-called frequency instability is depicted by the fluctuations in the period of the voltage. The situation is depicted in Fig. 1.[1]

The impacts of oscillator noise and the causes of short-term instabilities have been described in many research works and tutorials like [4,8,12]. The short-term stability measures most frequently found on oscillator specification sheets is the two-sample deviation, also called Allan deviation, $\sigma_y^2(\tau)$ (an estimate will be denoted by $s_y^2(\tau)$).

The Allan deviation and the modified Allan deviation have proved their adequacy in characterising frequency phase and instabilities. These easy-to-compute variances converge for all noise processes observed in precision frequency sources, have a straightforward relationship to power law spectral density of noise processes, and are faster and more accurate in than the FFT [13].

The estimates of these variances, for a given calibration time τ and for a m-data series of phase

[1] A similar example was provided by Prof. Eva Ferre-Pikal (University of Wyoming) and used by Vig in [8].

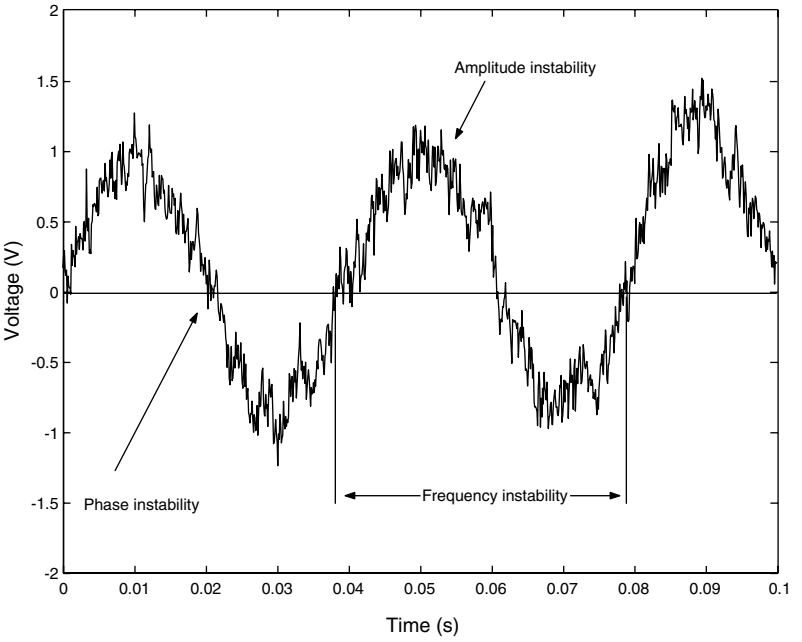

Fig. 1. Simulated types of instabilities in a 25 Hz sinusoidal output with additive noise. The noise process has a power spectral density proportional to the inverse of the frequency (flicker phase modulation). Fluctuations in the zero crossings of the voltage point to the phase instability. The so-called frequency instability is depicted by the fluctuations in the period of the voltage.

differences between the device under test and the reference x, are given by Eqs. (8) and (9), [6,14]

$$\hat{\sigma}_y^2(\tau) \triangleq s_y^2(\tau, m) = \frac{1}{2(m-1)} \sum_{j=2}^{m} \left(\bar{y}_j - \bar{y}_{j-1}\right)^2 = \frac{1}{2\tau^2(m-1)} \sum_{j=2}^{m} \left[\Delta_\tau^2 x(j\tau)\right]^2, \tag{8}$$

$$\hat{\mathrm{mod}}\,\sigma_y^2(\tau) \triangleq \mathrm{mod}\, s_y^2(\tau, m) = \frac{1}{2\tau^2} \langle \Delta_\tau^2 \bar{x} \rangle^2, \tag{9}$$

where the bar over x denotes the average in the time interval τ (averaging time), and $\Delta_\tau^2 x = x_{i+2} - 2x_{i+1} + x_i$, is the so called second difference of x [14]. The fractional frequency deviation is the relative phase difference in an interval τ. It is defined by Eq. (10)

$$\bar{y} = \frac{1}{\tau} \int_{t-\tau}^{t} y(s)\mathrm{d}s = \frac{x(t) - x(t-\tau)}{\tau} = \frac{\Delta_\tau x(t)}{\tau}. \tag{10}$$

Non-classical statistics estimators, defined in Eqs. (8) and (9), give an average dispersion of the fractional frequency deviation due to the noise processes coupled to the oscillator. As a consequence time domain instability (two-sample variance) is related to the power spectral density of the noise via [6]

$$s_y^2(\tau) = \frac{2}{(\pi v_0 \tau)^2} \int_0^{f_\mathrm{h}} S_\phi(f) \sin^4(\pi f \tau)\mathrm{d}f, \tag{11}$$

where v_0 is the carrier frequency, f is the Fourier frequency (the variable), and f_h is the band-width of the measurement system. $S_\phi(f)$ is the spectral density of phase deviations, which is in turn related to the spectral density of fractional frequency deviations via [6]

$$S_\phi(f) = \frac{v_0^2}{f^2} S_y(f). \tag{12}$$

The classical power-law noise model is a sum of the five common spectral densities. The model can be described by the one-sided phase spectral density $S_\phi(f)$ via [15,14]

$$S_\phi(f) = \frac{v_0^2}{f^2} \sum_{\alpha=-2}^{2} h_\alpha f^\alpha = v_0^2 \sum_{\beta=0}^{4} h_\beta f^\beta \tag{13}$$

for $0 \leqslant f \leqslant f_\mathrm{h}$. Where, again, f_h is the high-frequency cut-off of the measurement system (the band-width); h_α and h_β are constants which represent, respectively, the independent characteristic models of oscillator frequency and phase noise [5,15,14]. For integer values, the approximate expression is

$$s_y(\tau) \sim \tau^{\mu/2}, \tag{14}$$

where $\mu = -\alpha - 1$, for $-3 \leqslant \alpha \leqslant 1$; and $\mu \approx -2$ for $\alpha \geqslant 1$. In the case of the modified Allan deviation can be approximated via

$$\mathrm{mod}\, s_y(\tau) \sim \tau^{\mu'}. \tag{15}$$

Hereinafter we use Eqs. (14) and (15) for characterising noise.

3.2. Characterisation of the stability in the time domain

Eqs. (14) and (15) are used to make the graphical representation of $s_y(\tau)$ vs. τ, and allow us to infer the noise processes which causes frequency instability by means of measuring the slope in a log–log graph [6,16]. Table 1 shows the experimental criteria adopted. In the second column of the modified Allan variance two different criteria have been considered, according to [6,13], respectively. We have used the notation in [6,13] for $\mu/2$ and μ', respectively.

In order to adopt an experimental criteria, the five noise processes have been have been simulated. The results, depicted in Fig. 2, follow the criteria depicted in the second column of the modified Allan variance, in Table 1. Each data sequence contains

Table 1
The five noise processes characterized by the time and frequency domain slopes

Noise process	$S_y(f)$	$S_\phi(f)$	s $\hat{\sigma}_y(\tau) \sim \lvert\tau\rvert^{\frac{\mu}{2}}$	$\mathrm{mod}\, s$ $\hat{\sigma}_y(\tau) \sim \lvert\tau\rvert^{\mu'}$
	α	$\beta = \alpha - 2$	$\frac{\mu}{2}$	μ'
Random walk freq. mod.	−2	−4	0.5	1 (0.5)
Flicker freq. mod.	−1	−3	0	0 (0)
White freq. mod.	0	−2	−0.5	−1 (−0.5)
Flicker phase mod.	1	−1	−1	−2 (−1)
White phase mod.	2	0	−1	−3 (−1.5)

The Allan deviation is denoted by s and the modified deviation by $\mathrm{mod}\, s$.

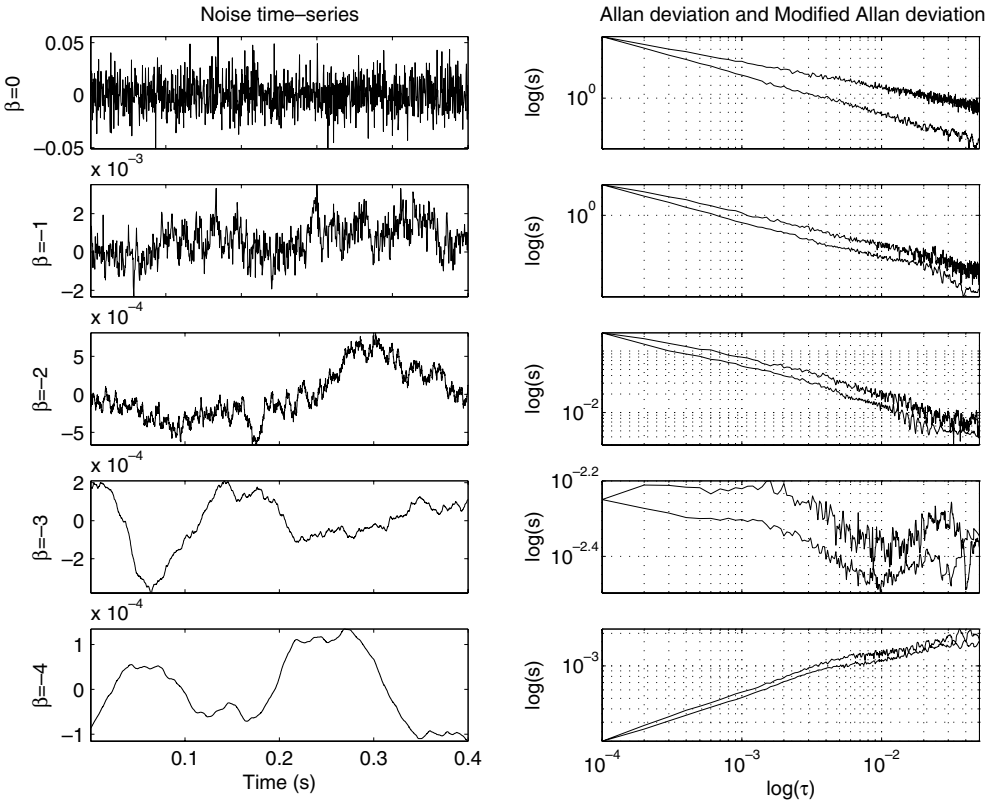

Fig. 2. Characterisation of the five noise processes depending of the power spectral laws.

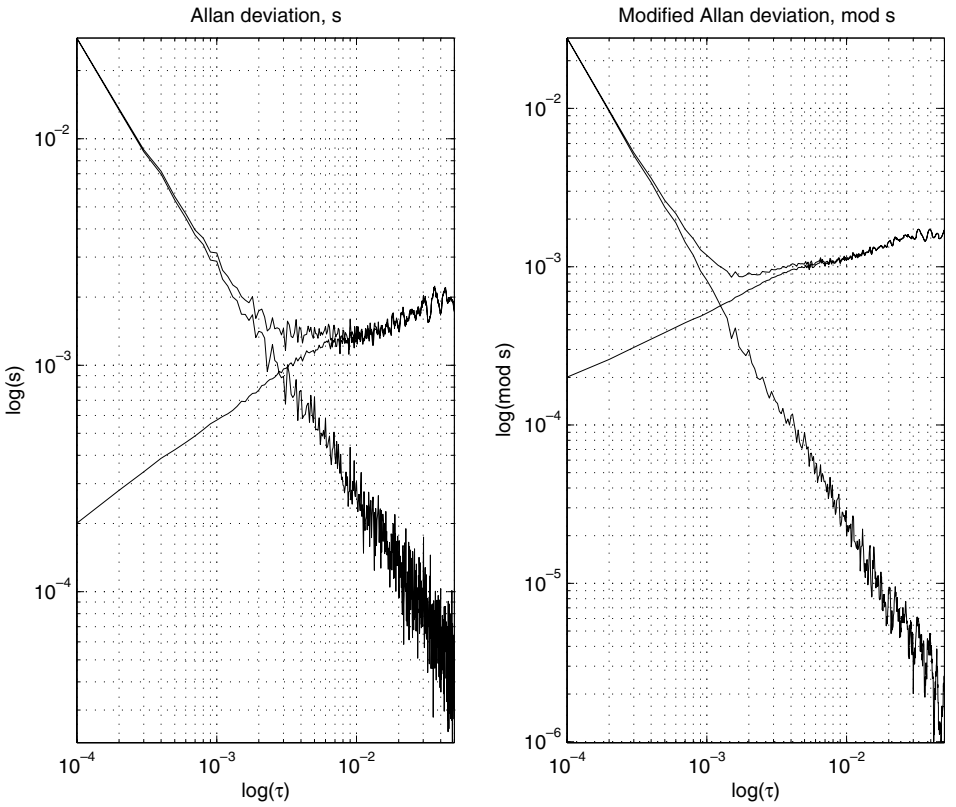

Fig. 3. Noise processes corresponding to $\beta = 0$ and $\beta = -4$. Situation of changing slope.

4096 points for a time resolution of $\tau = 10^{-4}$ s. Allan deviation graphs have been depicted for averaging times of $\tau = n \times \tau_0$, with $n \in [1, 500]$.

In many practical situations two or more noise processes simultaneously affect clocks performance. In these cases the upper enveloping curve determines the noise process coupled to the oscillator. If the individual variance curves cross each other, it is possible to see where the slope changes, for a time-series which includes several types of noise [7]. This situation is shown in Figs. 3 and 4.

In Fig. 3, the individual variance curves cross. So the enveloping curve characterizes the short-term instability. By the contrary, in Fig. 4 the $\beta = 0$ noise process has a variance greater than the $\beta = -4$ process.

4. Experimental results

4.1. Uncertainty calculations

A function generator, the device under test, is set up (from the front panel) to deliver a 1.1 (Hz) TTL signal. The experimental arrangement is depicted in Fig. 5. The time interval counter and a GPS receiver have been connected via GPIB to the computer. Data points are captured every 1 (s).

Fig. 6 shows the time-series resulting from the processing. Each measurement cycle corresponds to 1 (s). The bottom graph corresponds to the instantaneous phase-deviation series, which comprises $m = 898$ data. These data are the result of filtering the spiky time-series of phase differences, and are used to perform the calibration. They are supposed to be corrupted by white noise, with a rectangular probability density function.

Table 2 summarizes the results of the evaluation of the Type B standard uncertainty. It is an ordered arrangement of the quantities, estimates standard uncertainties, sensitivity coefficients and uncertainty contributions. It has been reported under the assumption of a rectangular (uniform) probability distribution of the magnitudes X_i (see the factor $\sqrt{3}$ in the particular uncertainties). The rightmost column has been rounded according to the resolution of the electronic counter.

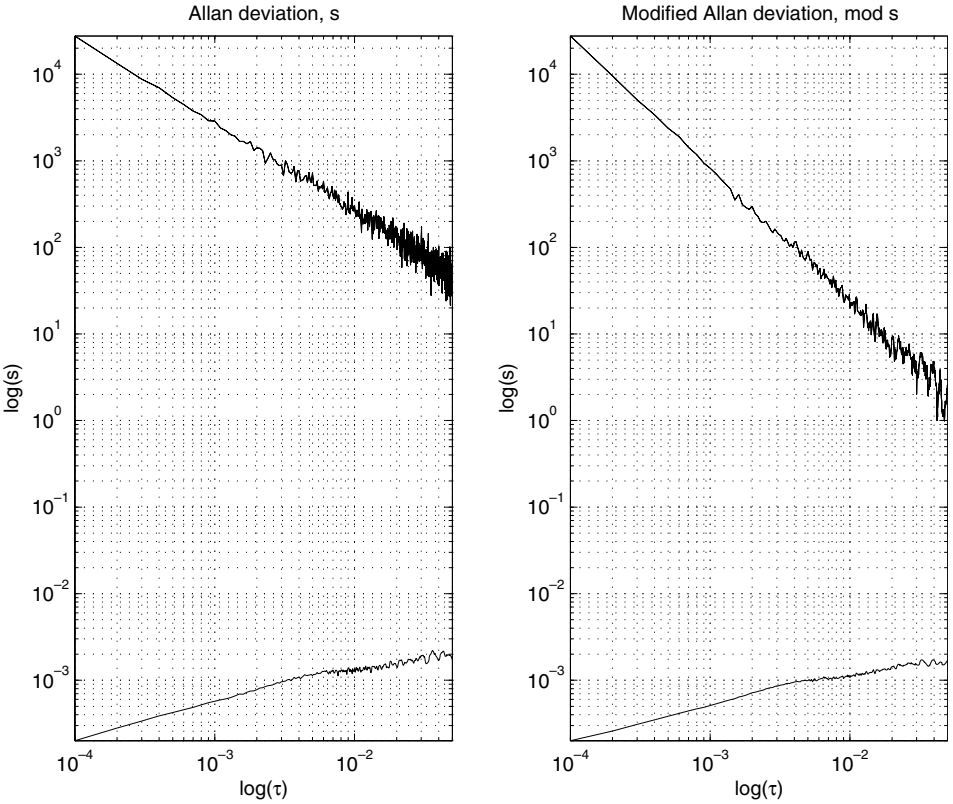

Fig. 4. Noise processes corresponding to $\beta = 0$ and $\beta = -4$. The upper noise process is the enveloping curve.

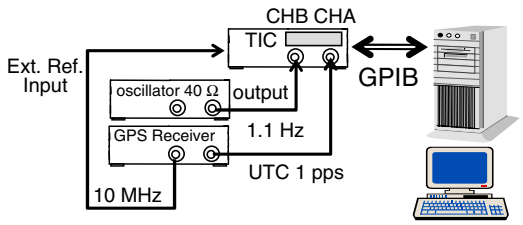

Fig. 5. Experimental arrangement.

The expression for the standard uncertainty is obtained from Eq. (16)

$$u^2(z) = 2 \times \sum_{i=1}^{N} u_i^2(z) + \frac{\sigma^2}{m}, \tag{16}$$

where the double factor is associated to the phase differences. Type A variance, $\frac{\sigma^2}{m}$, associated to the time-series, results 2×10^{-11} (s^2). Thus, Type A uncertainty results 5×10^{-6} (s).

The expanded uncertainty of the measurement is stated as the standard uncertainty multiplied by the coverage factor $k = 2$, which for a normal distribution attributed to the measurand corresponds to a coverage probability of approximately 0.95. Type B uncertainty is 2×10^{-7}. Including the contribution of Type A, the reported result of the measurement is $f_{\text{meas}} = 1.097493 \pm 0.000005$ (Hz), for measurement time of 898 (s).

4.2. Testing for white noise

The ratio of the classical variance to the Allan variance provides a primary test for white noise. This quantity (7.484×10^{-4}) is less than $1 + 1/\sqrt{m} \simeq 1.033$; thus it is probably safe to assume that the data set is dominated by white noise, and the classical statistical approach can safely be used. Failure of the test does not necessarily indicate the presence of non-white noise [9]. Fig. 7 shows the log–log curves of the Allan deviation and the modified Allan deviation vs. the calibration period, τ.

Measures of the slopes over the log–log graphs in Fig. 7 offer the results -1 and -1.5 for $\log(s)$ vs.

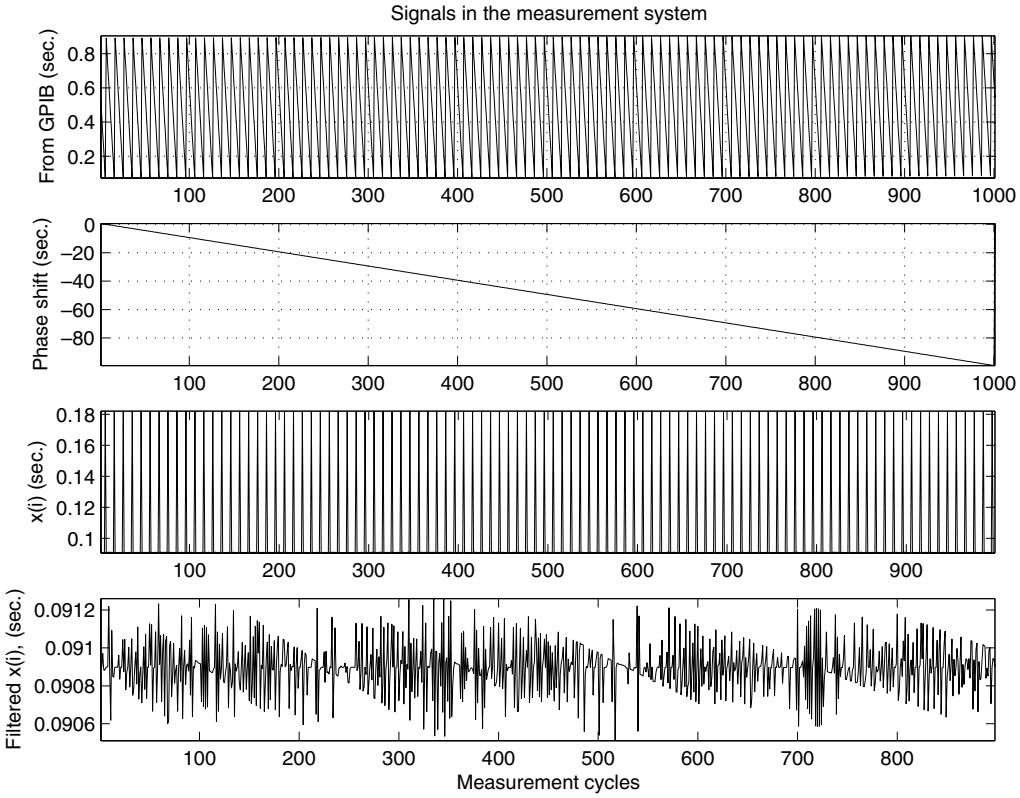

Fig. 6. Signals in the measurement chain. From top to bottom: original data from the time interval counter and the GPIB interface, accumulated phase shift, spiky phase differences, filtered phase differences.

Table 2
Sources of the Type B uncertainty assuming white noise

(TIC) HM8122 magnitude description	Value (ns)	Std. uncertainty (ns) $u(x_i)$	Contribution (ns) $u_i(z) = c_i \times u(x_i)$
X_1 (± 1 ext. clock) (GPS receiver)	100	$\frac{100}{\sqrt{3}}$	70
X_2 (time base error) (GPS clock's accuracy)	100	$\frac{100}{\sqrt{3}}$	70
X_3 (jitter)	5	$\frac{5}{\sqrt{3}}$	4
X_4 (systematic error)	<4	$\frac{4}{\sqrt{3}}$	3
X_5 (resolution)	100	$\frac{50}{\sqrt{3}}$	4
GPS receiver HM8125			
X_6 (accuracy)	100	$\frac{100}{\sqrt{3}}$	70
X_7 (jitter)	5	$\frac{5}{\sqrt{3}}$	4
Averaging time (measurement system)			
X_8	6	6	0.5
$u^2(x_8) = u^2(x_6) + u^2(x_7)$			

$\log(\tau)$, and $\log(\mathrm{mod}\, s)$ vs. $\log(\tau)$, respectively; which indicate that a white phase modulation process is coupled to the frequency source under test (see Table 1).

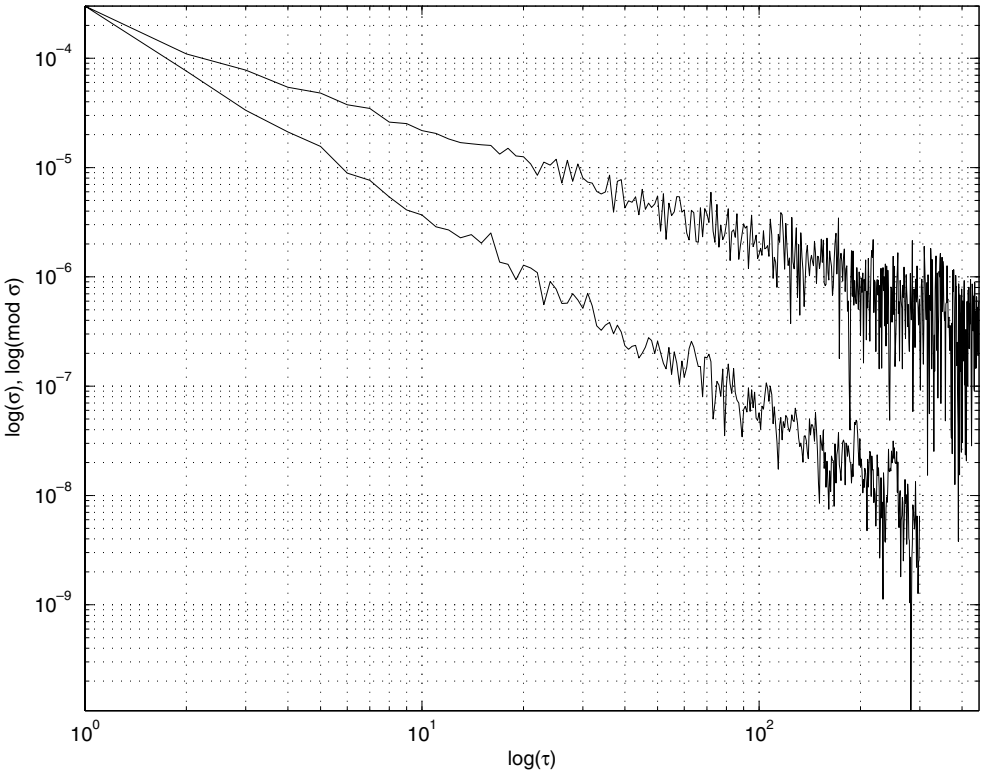

Fig. 7. Allan variance, s (upper) and, modified Allan variance mod s (lower) log–log curves. The final calibration period is $\tau = 500 \times \tau_0$ for $\tau_0 = 1$ s.

5. Conclusion

This paper shows how to deal with frequency calibrations using incompletely characterised instruments. The calibration of a function generator has been taken as an example. The different uncertainties have been calculated under the hypothesis of a rectangular distribution of errors. The reported standard uncertainty is dominated by the Type A uncertainty. The Type B uncertainty of the frequency is one order of magnitude less than the Type A uncertainty.

Short-term instability estimators has been tested using simulated noise processes. A result regarding the simultaneous action of two noise processes has been reported, showing a low-variance noise masked by a higher variance one. Then, once the non-classical estimators have been assessed, a white noise test has been applied based on the calculation of the classical to non-classical variance ratio, and supported by the direct measurement of the slopes on the graphs which depict the Allan deviation and the modified Allan deviation vs. the measurement time.

Acknowledgements

The authors would like to thank the Spanish Ministry of Education and Science for funding the project DPI2003-00878 which involves noise processes modelling and time-frequency calibration.

References

[1] M. Lombardi, An introduction to frequency calibration: Part I, Cal Lab The International Journal of Metrology (January–February) (1996) 17–28.
[2] M. Lombardi, An introduction to frequency calibration: Part II, Cal Lab The International Journal of Metrology (March–April) (1996) 28–34.
[3] M. Lombardi, Traceability in time and frequency metrology, Cal Lab The International Journal of Metrology (September–October) (1999) 33–44.
[4] D. Howe, D. Allan, J. Barnes, Properties of oscillator signals and measurement methods, Technical Report, Time and Frequency Division, National Institute of Standards and Technology, 1999.
[5] D. Allan, Time and frequency (time-domain) characterization, estimation, and prediction of precision clocks and oscillators, IEEE Transactions on Ultrasonics, Ferroelectrics, and Frequency Control 34 (752) (1987) 647–654.

[6] J. Rutman, F. Walls, Characterization of frequency stability in precision frequency sources, Proceedings of IEEE 79 (7) (1991) 952–960.
[7] F. Vernotte, Oscillator noise analysis: multivariance measurement, IEEE Transactions on Instrumentation and Measurement 42 (2) (1993) 342–350.
[8] J.R. Vig, A tutorial for frequency control and timing applications, Technical Report AD-A328861 SLCET-TR-88-1 (Rev.8.4.3), US Army Communications-Electronics Command. Attn: AMSEL-RD-C2-PT, Fort Monmouth, NJ 07703, USA, approved for public release (January 2001).
[9] Fluke, Calibration: Philosophy in Practice, second ed., vol. Library of Congress Catalogue Card Number: 93-90764, Fluke Corporation ISBN 0-9638650-0-5, 1994.
[10] E.T. Force, Expression of the uncertainty of measurement in calibration EA-4/02, EA European co-operation for Accreditation (ISO), 1999.
[11] R. Swarup, P. Negi, R. Mendiratta, Estimation of uncertainty in impedance measurement at narrow and broadband microwave frequencies, Measurement 2 (33) (2003) 55–66.
[12] D. Sullivan, D. Allan, D. Howe, F. Walls, Characterization of clocks and oscillators, NIST Tech Note 868 (1337), BIN: 868, 1990.
[13] P. Lesage, T. Ayi, Characterisation or frequency stability: analysis of the modified Allan variance and properties of its estimate, IEEE Transactions on Instrumentation and Measurement IM-33 (4) (1984) 332–336.
[14] C. Greenhall, Frequency stability review, TDA progress report 42-88, Communications Systems Research Section, Jet Propulsion Laboratory 1 (1) (1988) 200–212.
[15] IEEE standard definitions of physical quantities for fundamental frequency and time metrology, Technical Report IEEE Std 1139-1988, The Institute of Electrical and Electronics Engineers, Inc., 345 East 47th Street, New York, 10017, USA, April 1988.
[16] G. Wei, Estimations of frequency and its drift rate, IEEE Transactions on Instrumentation and Measurement 46 (1) (1997) 79–82.